

A Wireless Communication Link for a Miniature, Implantable Neuromodulation System

by

Scott Matthew McCuen

S.B. EECS, MIT (2018)

Submitted to the Department of Electrical Engineering and Computer
Science

in partial fulfillment of the requirements for the degree of

Master of Engineering in Electrical Engineering and Computer Science

at the

MASSACHUSETTS INSTITUTE OF TECHNOLOGY

June 2019

© Massachusetts Institute of Technology 2019. All rights reserved.

Author
Department of Electrical Engineering and Computer Science
May 24, 2019

Certified by.....
Charles G. Sodini
LeBel Professor of Electrical Engineering
Thesis Supervisor

Certified by.....
Carlos Segura
Draper Senior Member of Technical Staff
Thesis Supervisor

Accepted by
Katrina LaCurts
Chair, Master of Engineering Thesis Committee

A Wireless Communication Link for a Miniature, Implantable Neuromodulation System

by

Scott Matthew McCuen

Submitted to the Department of Electrical Engineering and Computer Science
on May 24, 2019, in partial fulfillment of the
requirements for the degree of
Master of Engineering in Electrical Engineering and Computer Science

Abstract

Neuromodulation is a promising treatment for a variety of otherwise intractable medical conditions. Current neuromodulation devices are large, single-purpose, and limited in functionality. Draper developed a novel, implantable neuromodulation system to address these shortcomings. The system is wireless and networked, and it consists of one external transceiver and multiple implants. The primary contributions of this project included demonstration of stimulation with an implant through a wired interface, demonstration and characterization of a Bluetooth Low Energy (BLE) connection with an implant, and demonstration of stimulation on an implant from a command sent through BLE. The primary challenges of the project were to understand, debug, and validate a complex embedded system. When evaluating BLE performance, a BLE connection interval of 10ms led to a mean latency of 21.2ms with a standard deviation of 6.9ms. The BLE hardware consumed 0.66mW when idle and 3.5mW when connected.

Thesis Supervisor: Charles G. Sodini
Title: LeBel Professor of Electrical Engineering

Thesis Supervisor: Carlos Segura
Title: Draper Senior Member of Technical Staff

Acknowledgments

This project is not mine alone. Rather, it is the work of a whole team of people. I would like to thank some of them here.

I would like to thank Carlos Segura, Professor Sodini, and Jesse Wheeler for their guidance throughout this project. Carlos and Jesse gave me the opportunity to work on an incredible project, and I am grateful for their support and mentorship over the last year. It was a pleasure to work with both of them, and I hope I have made a valuable contribution to this project.

I would also like to thank Alejandro Miranda, Jake Hellman, Matt Muresan, Andrew Czarnecki, Mark Lutian, and Elliot Greenwald for their technical support throughout this project. All of these engineers took time out of their days to answer my many questions and help me move the project forward, and for that I am endlessly thankful.

Thank you to Kathleen Melvin, Martha Porter, and Sheila Hemami for running the MIT 6-A program and the Draper Fellows program.

I would like to thank my family for supporting me in every way possible from the very beginning. They have provided me with a world of opportunities, and I would not be here without them.

Lastly, I would like to thank my girlfriend for never losing faith in me through all of the highs and lows and encouraging me to keep moving. The challenges of the past year would have felt insurmountable without you, and I am forever grateful to you for sticking by my side.

Contents

| | | |
|----------|--|-----------|
| 1 | Introduction | 13 |
| 2 | Neuromodulation | 15 |
| 2.1 | Definition of Neuromodulation | 15 |
| 2.2 | History of Neuromodulation | 15 |
| 2.3 | Current Neuromodulation Technologies and Research | 16 |
| 2.4 | Shortcomings of Current Neuromodulation Technologies | 17 |
| 2.4.1 | Implanted Volume | 17 |
| 2.4.2 | Architecture | 18 |
| 2.4.3 | Limited Functionality | 18 |
| 3 | An Advanced Implant System | 19 |
| 3.1 | Overview | 19 |
| 3.2 | Hardware | 22 |
| 3.2.1 | Implant | 22 |
| 3.2.2 | External Transceiver | 26 |
| 3.3 | Use Cases | 27 |
| 4 | Contributions | 29 |
| 4.1 | Stimulation | 29 |
| 4.1.1 | Stimulation FPGA Simulation | 29 |
| 4.1.2 | Configuring the Stimulation Chip | 30 |
| 4.1.3 | Configuring the Stimulation Cross-Point Switch | 31 |

| | | |
|----------|---|-----------|
| 4.2 | Wireless Stimulation | 32 |
| 4.2.1 | BLE Connection on Development Boards | 32 |
| 4.2.2 | BLE Connection with the Implant | 33 |
| 4.2.3 | SPI Connection with BLE | 34 |
| 5 | Measurements | 35 |
| 5.1 | Stimulation Latency | 35 |
| 5.2 | Power Consumption | 36 |
| 5.2.1 | Power Consumption by Component | 37 |
| 5.2.2 | Power Consumption with Varying Stimulation Parameters | 38 |
| 5.2.3 | Power Consumption with Varying BLE Connection Intervals | 39 |
| 6 | Future Work | 41 |
| 6.1 | Security | 41 |
| 6.2 | Alternatives to BLE | 42 |
| 6.3 | Reducing Power Consumption | 43 |

List of Tables

| | | |
|-----|---|----|
| 3.1 | Major Components in the Implant | 27 |
| 5.1 | Latency with Varying Connection Intervals | 36 |
| 5.2 | Power Consumption by Component (Idle State) | 38 |
| 5.3 | Power Consumption with Varying Stimulation Parameters | 40 |
| 5.4 | Power Consumption with Varying BLE Connection Intervals | 40 |

List of Figures

| | | |
|-----|--|----|
| 2-1 | Examples of IPG-based neuromodulation devices. Left: NeuroPace RNS DBS system [1]. Right: Nevro HF10 SCS system [2]. | 18 |
| 3-1 | Renderings of a previous wired, networked Draper implant. (Rendering by Draper) | 20 |
| 3-2 | Diagram of the connections (data and power) between the implants and the external transceiver. | 21 |
| 3-3 | Rendering of four implants implanted in a forearm with the external transceiver cuff overlaid. (Rendering by Draper) | 21 |
| 3-4 | Images of the packaged implant. [3] | 22 |
| 3-5 | Photo of the implant development board. Actual implant is in the light green portion of the board. | 23 |
| 3-6 | Simplified hardware diagram of the external transceiver and implant. | 23 |
| 3-7 | Annotated waveform of current stimulation from Stim Chip. | 25 |
| 3-8 | A simplified version of the external transceiver and the implant. | 27 |
| 3-9 | Renderings of the implanted system. (Rendering by Draper) | 28 |
| 4-1 | Oscilloscope shot of a typical stimulation with two active channels. | 31 |
| 5-1 | Latency Distributions for Various Connection Intervals | 36 |
| 5-2 | Power consumption per channel at various stimulation frequencies and amplitudes | 39 |
| 6-1 | Comparison of power consumption and data rate of various wireless protocols | 42 |

Chapter 1

Introduction

The goal of this work was to develop and demonstrate a wireless communication link to an implantable neuromodulation system using Bluetooth Low Energy (BLE). Neuromodulation is a promising medical intervention in which electrical stimulation is applied to select parts of the nervous system including peripheral nerves and the brain. Neuromodulation exists in many forms, and modern devices successfully treat epilepsy, Parkinson's disease, chronic pain, and depression.

The neuromodulation system used in this work improves upon existing neuromodulation systems with its smaller size, networked architecture, and flexibility. The system can be wirelessly reconfigured to provide a wide range of closed-loop therapies without adding new hardware. The primary contributions of this project included demonstration of stimulation with the implant through a wired interface, demonstration and characterization of a BLE connection with the implant, and demonstration of stimulation on the implant from a command sent through BLE.

In this work, I first establish the motivation for this project and provide background information on neuromodulation including its history, existing neuromodulation technologies, and the shortcomings of existing technologies. As a response to these shortcomings, I introduce a novel neuromodulation implant and describe it in detail, including the function of all major components. I proceed to outline the primary contributions of this work to the neuromodulation implant project and provide measurements of key parameters of the implant including latency and power

consumption. Lastly, I offer some suggestions for future work on the implant.

Chapter 2

Neuromodulation

2.1 Definition of Neuromodulation

Neuromodulation is the “process of inhibition, stimulation, modification, regulation or therapeutic alteration of activity, either electrically or chemically, in the central, peripheral or autonomic nervous systems” [4]. For the purposes of this project, neuromodulation will refer exclusively to electrical stimulation of the nervous system.

Neuromodulation relies on the knowledge that the nervous system controls the entire body, and the way in which nerves stimulate parts of the body determines how they operate. If a part of the body is not working normally, it may be possible to correct the behavior of that part by changing the way in which it is stimulated.

2.2 History of Neuromodulation

The concept of applying electricity to the human body for the purpose of treating illness has existed for thousands of years. In 15 AD, the physician of Emperor Tiberius observed a slave who was suffering from painful gout inadvertently alleviate his pain by stepping on an electric torpedo fish. Using this knowledge, he prescribed electric fish therapy to future patients suffering from chronic pain [4].

Neuromodulation in its modern form started with simple forms of deep brain stimulation (DBS) and Norman Shealy’s spinal cord stimulation (SCS) to relieve

chronic pain [5]. Shealy utilized modified stimulators from Medtronic intended to treat hypertension, and Medtronic soon began manufacturing stimulators specifically for SCS. Early forms of DBS and SCS both focused on pain relief, but DBS pivoted to treatment of movement disorders in 1980 with Brice and McLellan [6].

Interest in neuromodulation persisted through the next few decades, and neurosurgeons began to favor stimulation as a lower risk alternative to lesions in patients with severe movement disorders.

2.3 Current Neuromodulation Technologies and Research

Neuromodulation is effective for treating a variety of otherwise intractable conditions, and new applications surface regularly. Many forms of neuromodulation are experimental and are only used in research, but some have been refined enough to earn FDA approval for use in humans.

A few of the most common forms of neuromodulation today are vagus nerve stimulation (VNS), deep brain stimulation, and spinal cord stimulation. Among the many other forms are sacral nerve stimulation, gastric electrical stimulation, carotid artery stimulation, occipital nerve stimulation, cochlear implants, and diaphragm pacing [7].

Devices for the most common neuromodulation therapies are manufactured by a number of medical device companies. LivaNova offers a VNS stimulator to treat seizures in patients with severe epilepsy [8]. Abbott, Medtronic, and Neuropace offer DBS systems to treat Parkinson’s disease, epilepsy, and other movement disorders [9, 10, 1]. Nevro, Boston Scientific, Medtronic, and Abbott all offer SCS systems for pain relief [2, 11, 12, 13].

In addition to industry, many research institutions work on neuromodulation devices. The Defense Advanced Research Projects Agency (DARPA) oversees a variety of programs in neurotechnology. Notably, the Systems-Based Neurotechnology for Emerging Therapies (SUBNETS) program aims to develop targeted therapies for

patients with neuropsychiatric disorders like major depression, post-traumatic stress disorder, and addiction [14]. The National Institutes of Health (NIH) funds numerous research efforts as well. The Stimulating Peripheral Activity to Relieve Conditions (SPARC) program coordinates a variety of research efforts to understand interactions between nerves and organs throughout the body. The ultimate goal of the program is to develop “precise treatment of diseases and conditions for which conventional therapies fall short” [15].

2.4 Shortcomings of Current Neuromodulation Technologies

2.4.1 Implanted Volume

Implanting a device in the body is inherently invasive. The larger a device is, the more challenging it is to implant in a body. Most current neuromodulation implants have volumes of more than 10 cm^3 and are implanted in the torso. Medtronic, a leading manufacturer of medical implants, offers devices in the range of 40 to 60 cm^3 , and their more complex devices are even larger.

Most neuromodulation devices use roughly the same form factor: a titanium enclosure containing electronics and a power source (often referred to as an implantable pulse generator or IPG) with one or more insulated leads routed to one or more points of stimulation. This form factor is effectively the same as a pacemaker, and it has remained largely the same since the beginning of neuromodulation. Figure 2-1 shows two standard form factor IPG devices.

In order to reach small anatomical targets, current devices use long leads extending from the implant. For example, DBS systems often have a pulse generator placed in the torso with leads running up the neck and into brain structures. This introduces risks of mechanical device failure and consequently patient safety. In order to overcome these challenges and expand the use of neuromodulation devices, we must develop smaller systems with wireless connections.



Figure 2-1: Examples of IPG-based neuromodulation devices. Left: NeuroPace RNS DBS system [1]. Right: Nevro HF10 SCS system [2].

2.4.2 Architecture

Typically, an implant offers only one form of therapy in a specific location. While these single-purpose devices are effective in certain cases, they cannot offer therapy distributed among different targets in the body. For example, two DBS implants are required for bilateral stimulation of the brain. However, existing devices are not networked and cannot coordinate therapies. An architecture that allows for coordination of stimulation and recording across multiple implants would permit more effective therapies for complex diseases.

2.4.3 Limited Functionality

Most devices offer only one form of open-loop therapy and cannot be reconfigured easily to record and stimulate in new ways. Only a few devices (e.g. NeuroPace RNS) offer closed-loop, responsive therapy. They rely upon real-time processing within the implant, which is limited by computational resources. A low-latency, wireless link could enable real-time processing by an external system, allowing for more effective therapies.

Chapter 3

An Advanced Implant System

3.1 Overview

To address the shortcomings of neuromodulation devices, Draper has designed a number of miniature, wireless, networked neuromodulation systems. The system used in this work was designed to use Bluetooth Low Energy as a wireless communication link. The primary goal of this thesis was to develop the Bluetooth Low Energy link and demonstrate wireless programming for stimulation.

Draper has developed previous neuromodulation implants that are networked through wired leads. For example, one system was designed to control a motorized prosthetic arm and provide sensory feedback through connections to residual muscles and nerves in amputees. In this system, a central hub, comparable in size to a traditional neuromodulation implant, communicated with and powered multiple satellites along a common bus. Each satellite recorded and stimulated nerves and muscles in a different part of the subject's arm. This architecture improved upon previous implants by coordinating recording and stimulation across multiple locations within the body and reducing the number of implanted leads. Renderings of this system are shown in Figure 3-1a and Figure 3-1b.

The current system takes a step beyond the wired, networked system by eliminating leads between the satellites and hub. An external transceiver (not implanted) wirelessly powers and communicates with multiple satellite implants. A block dia-

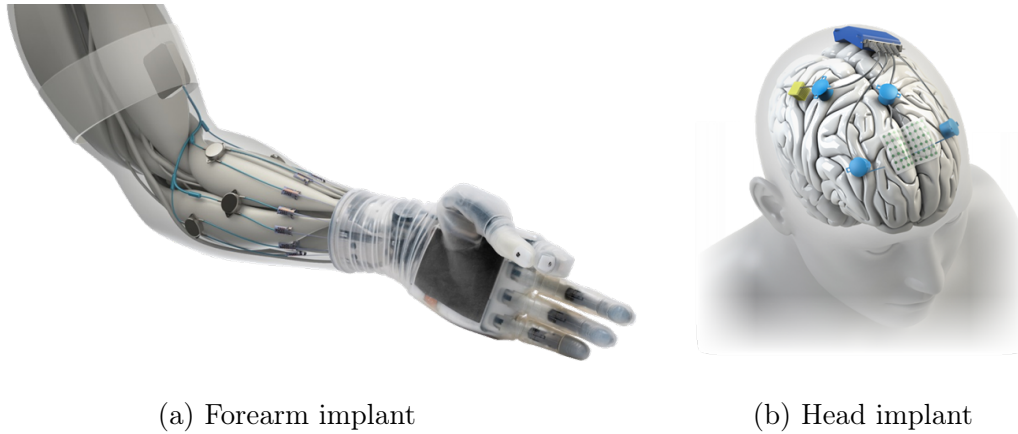


Figure 3-1: Renderings of a previous wired, networked Draper implant. (Rendering by Draper)

gram showing the connections between the implants and the external transceiver is shown in 3-2. A rendering of several implants in an arm with an external transceiver cuff overlaid is shown in Figure 3-3.

The neuromodulation system is low volume. Each implant is less than 2.3 cm^3 and, due to its small size, can be implanted closer to the point of stimulation than many other neuromodulation devices, potentially reducing the length of implanted leads. This makes the system less invasive than traditional IPG-based neurostimulators. Figure 3-4 shows the actual size of an implant.

The neuromodulation system is highly configurable. A single implant can support up to 32 electrodes, each of which can be configured in real time for both single-ended and differential stimulation and recording.

The system uses a distributed architecture, so it can adapt easily to a variety of use cases. Each implant can connect to a different set of electrodes, and each set of electrodes can have different characteristics. For example, one implant might connect to a Utah Array while another connects to a DBS probe [16]. Up to four implants can connect to a single external transceiver, enabling distributed therapy with 128 configurable electrodes.

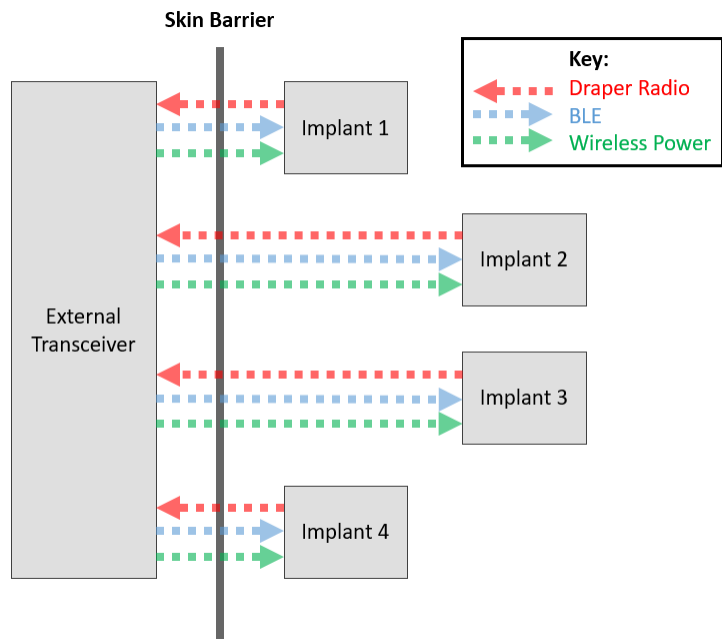
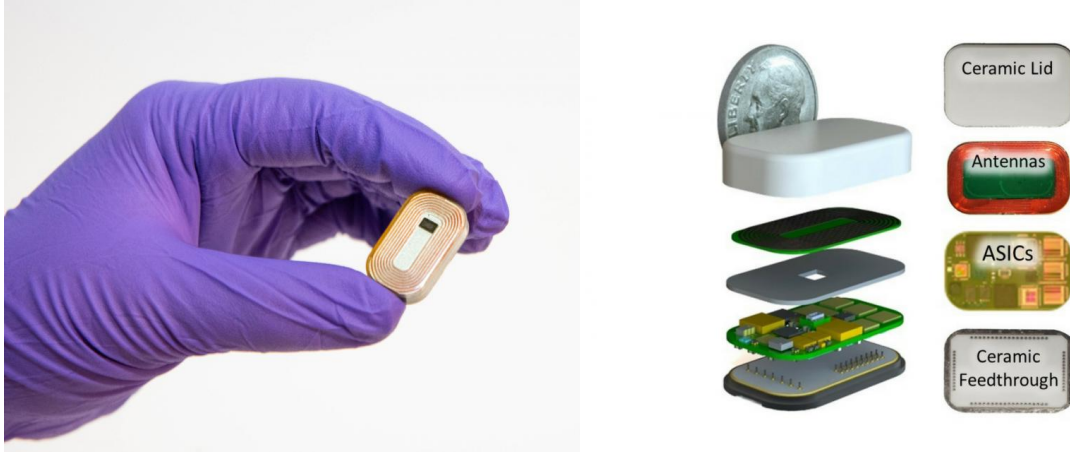


Figure 3-2: Diagram of the connections (data and power) between the implants and the external transceiver.



Figure 3-3: Rendering of four implants implanted in a forearm with the external transceiver cuff overlaid. (Rendering by Draper)



(a) Mock up of actual size

(b) Exploded view of layers

Figure 3-4: Images of the packaged implant. [3]

3.2 Hardware

This work used a development version of the implant and a number of break-out boards and is concerned only with the functionality of the system, not the form factor. Figure 3-6 shows a simplified hardware diagram of the major components in the implant and external transceiver.

3.2.1 Implant

The break-out board version of the implant contains all of the same hardware as the implantable version, but it makes every pin in the system easily accessible. The actual implant is in the center of the board and is designed to scale. If the implant were cut out of the breakout board, it would have all of the necessary connections and components to function on its own, other than the antennae for wireless power and communication and the electrodes. Figure 3-5 is a photo of the implant breakout board. The following sections provide more detail about each of the major components, and Table 3.1 summarizes the characteristics of each component.

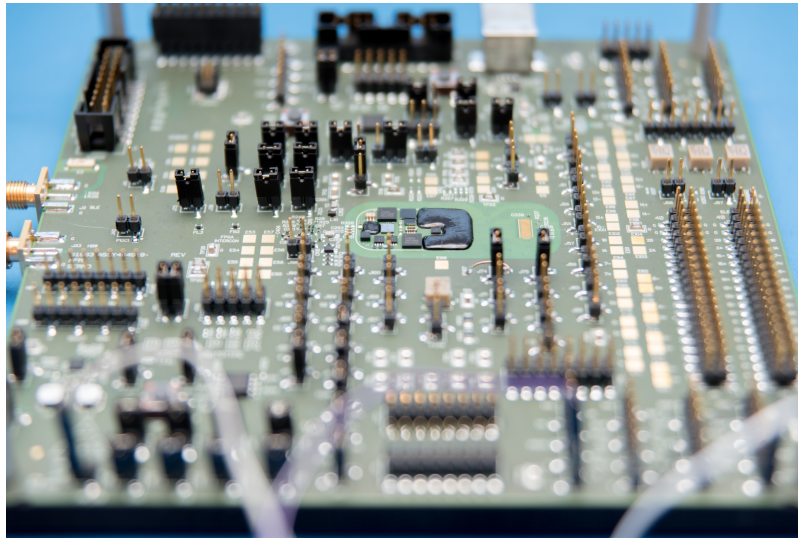


Figure 3-5: Photo of the implant development board. Actual implant is in the light green portion of the board.

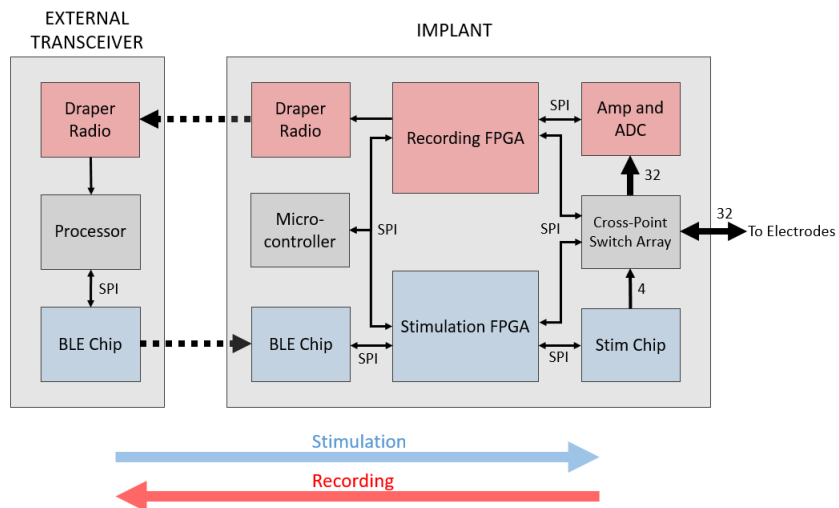


Figure 3-6: Simplified hardware diagram of the external transceiver and implant.

Bluetooth Low Energy Chip

The primary purpose of the Bluetooth Low Energy Chip (BLE Chip) is to receive commands from the external transceiver and forward them to configure stimulation and/or recording. This particular chip is ultra low power and designed around two ARM processors. An ARM Cortex-M0 runs the BLE stack and an ARM Cortex-M0 serves as the main processor. The BLE Chip is a SPI master to the Stimulation FPGA and the Recording FPGA.

Microcontroller

The microcontroller (MCU) on the implant serves primarily to send commands for recording and stimulation. This particular microcontroller uses an ARM Cortex-M0+ processor and is designed for ultra-low-power operation. The MCU on the implant operates with a 24 MHz crystal and drives a clock signal that is shared with the BLE Chip and the FPGAs. The MCU is a SPI master to both the Stimulation FPGA and Recording FPGA. Through these SPI connections, the MCU can send commands to the FPGAs to configure the Stimulation Chip, the amplifier and ADC chip, and the cross-point switches.

Stimulation and Recording FPGAs

The Stimulation FPGA and Recording FPGA serve as a bridge between the control/communication components (BLE chip, MCU, and Draper radio) and the stimulation and recording hardware (Stimulation chip, cross-point switches, Amplifier and ADC Chip). The two FPGAs are separate only due to size constraints on the implant. They essentially function as one larger FPGA. The Stimulation FPGA is a SPI slave to the MCU and the BLE Chip and is a SPI master to the Stimulation Chip and two cross-point switches. The Recording FPGA is also a SPI slave to the MCU and the BLE Chip and is a SPI master to the Amplifier and ADC Chip, the Draper Radio, and one cross-point switch.

Stimulation Chip

The stimulation chip (Stim Chip) is a custom Draper ASIC designed to deliver charge-balanced current stimulation on up to 4 channels. The maximum stimulation amplitude is 10 mA. The Stim Chip can send either a specific number of stimulation pulses (1 to 1024) or stimulate continuously. The anodic pulse width, cathodic pulse width, inter-phase delay, and inter-pulse delay are all programmable. The chip can be configured for both differential stimulation (between 2 electrodes) and single-ended stimulation (1 electrode to reference). In order to eliminate residual charge on electrodes following stimulation, the stimulation outputs can be automatically shorted to ground. Figure 3-7 shows the form of a stimulation pulse.

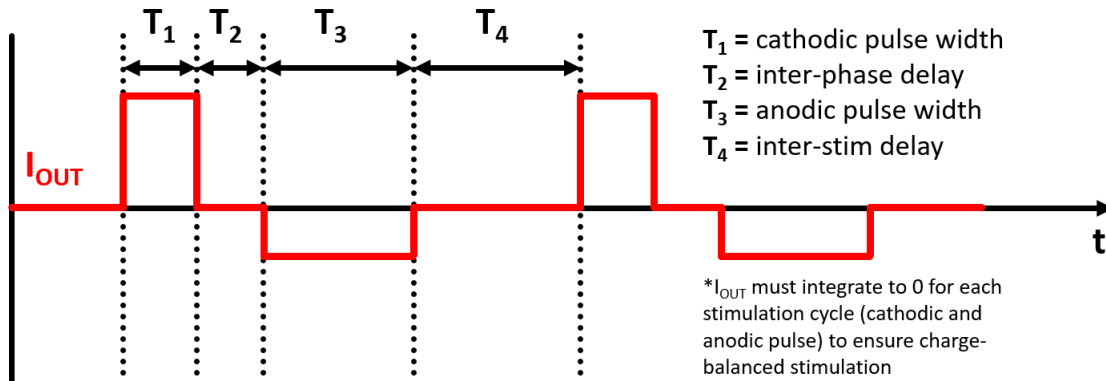


Figure 3-7: Annotated waveform of current stimulation from Stim Chip.

Cross-Point Switches

The cross-point switch array (CPS Array) enables the implant to easily change the configuration of stimulating and recording electrodes. The CPS array consists of 3 2x32 cross-point switches. Each switch has 32 electrode connections, 32 recording connections, and 2 analog input connections. Each electrode connection can be independently connected to its corresponding recording connection, and the two analog inputs can each be connected to any combination of electrodes. Two 2x32 cross-point switches act as a single 4x32 CPS to connect electrodes to the stimulation chip. This CPS array is a SPI slave to the Stimulation FPGA. Each stimulation line can connect to any combination of the 32 electrodes. The third CPS controls the connection of

electrodes to each of the 32 inputs of the Amplifier and ADC Chip . This CPS is a SPI slave to the Recording FPGA. Each CPS has a maximum transition time of 100 ns and a maximum on resistance of 100 ohms.

Amplifier and ADC Chip

The Amplifier and ADC Chip (Amp/ADC) is designed specifically for electrophysiology and can be configured to record on up to 32 channels at 30 kSamples/s on each channel. The 32 analog inputs feed into 16 differential amplifiers, and the chip incorporates bypass capacitors and ESD protection at the inputs to each amplifier. The upper bandwidth of the Amp/ADC is programmable from 100 Hz to 20 kHz, and the lower bandwidth is programmable from 0.1 Hz to 500 Hz. An analog multiplexer connects the output of each amplifier to a 1.05 Mbps, 16-bit ADC. The chip is configured through a SPI interface.

Draper Radio

The Draper Radio is a custom radio transmitter designed by Draper. This project focused on stimulation, so the Draper Radio was not used.

3.2.2 External Transceiver

Full-Featured Transceiver

In its final form, the external transceiver must receive data sent through the Draper Radio, send commands to the implant through BLE, and power the implant wirelessly. The external transceiver receives data from the Draper Radio with a software-defined radio and sends commands to the implant through BLE.

Simplified Transceiver

For the purposes of this project, which focuses on stimulation, the external transceiver's only function is to send commands to the implant through BLE. I developed a simpli-

Table 3.1: Major Components in the Implant

| Component | Abbreviation | Characteristics |
|--------------------------------------|--------------|--|
| Microcontroller | MCU | ARM-based Cortex-M0+ |
| Bluetooth Low Energy Microcontroller | BLE Chip | BLE 4.2 and 5.0, ARM Cortex-M3 and M0 |
| Stimulation FPGA | Stim FPGA | Ultra-low power |
| Recording FPGA | Rec FPGA | Ultra-low power |
| Draper Radio | Draper Radio | 20 Mbit/s, low power |
| Stimulation Chip | StimChip | 4 channels, single-ended and diff., 10mA per channel |
| Amplifier and ADC | Amp/ADC | 32 channels at 30kS/s, bipolar/monopolar, designed for electrophysiology |
| Cross-Point Switch (x3) | CPS array | 3 2x32 switches configured as one 4x32 switch and one 2x32 switch |

fied external transceiver consisting of a BLE development board and a microcontroller. A diagram representing this simplified external transceiver is shown in Figure 3-8.

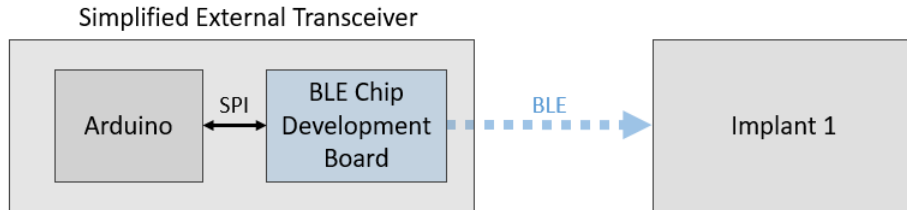
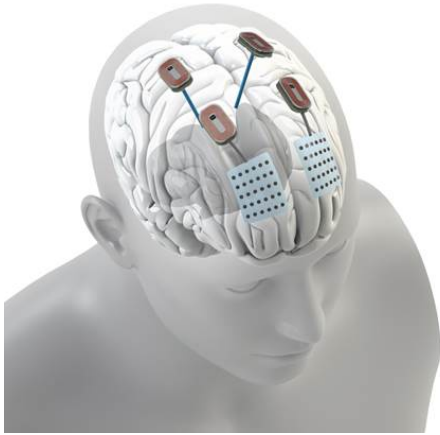


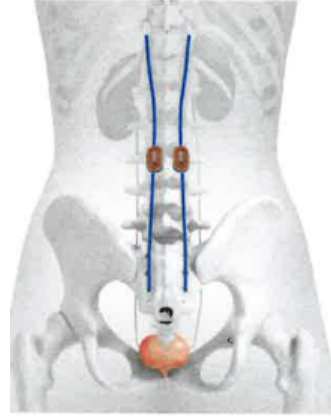
Figure 3-8: A simplified version of the external transceiver and the implant.

3.3 Use Cases

The neuromodulation system is designed to work in a variety of use cases. The system is well-suited to serve the same purpose as previous Draper neuromodulation systems implemented with wired networks. For example, the multiple implants can



(a) Head implant



(b) Back implant

Figure 3-9: Renderings of the implanted system. (Rendering by Draper)

be wirelessly connected to control and record feedback from a prosthetic limb. Its stimulation and recording capabilities and ability to reconfigure electrodes also allow the implant to replace most existing neuromodulation systems. The implant might be implanted in the head to record with ECoG arrays as shown in Figure 3-9a or implanted in the back to perform spinal cord stimulation as in Figure 3-9b.

Chapter 4

Contributions

4.1 Stimulation

The first goal of this project was to initiate stimulation with the Stim Chip by sending a command from the MCU. The MCU communicates with the Stim Chip and CPS indirectly through the Stimulation FPGA, so this stage required an in-depth understanding of each of these four components.

4.1.1 Stimulation FPGA Simulation

I initially focused on validating the operation of existing VHDL written for the Stimulation FPGA. In order to ensure correct operation of the Stimulation FPGA in a variety of conditions, I first tested its behavior in simulation. Previous contributors to the project set up a simulation of the Stimulation FPGA and the digital interfaces of several implant components. The simulated FPGA accepts manufactured SPI data as an input and responds with output signals to the Stim Chip and CPS.

Both FPGAs implement a "billboard" to keep track of the parameters for each peripheral device (Stim Chip, CPS, Amp, etc.). To update the parameters in a given part of the billboard, the MCU or BLE Chip sends a series of SPI messages to the FPGA. The messages flow through a FIFO and are handled by a "data manager." Part of each message specifies an address A within the billboard, and another part

specifies a number of slots n in the billboard. The data manager places the following n messages in slots A to $A + n - 1$. Different sequences of slots correspond to different parameters.

After the data manager places received SPI data into the billboard, a number of component "engines" read the data and format it appropriately to program the peripheral components. For example, the "Stim Chip Engine" packages data from the billboard into a bit sequence to send to the Stim Chip.

The Stim Chip contains 2 shift registers, accessed with 2 separate chip select lines, and each controls 2 channels of stimulation. Half of each shift register controls one channel, and half controls the other channel. A given register controls triggering of the channel, calibration, configuration of stimulation properties, configuration of timing properties, and configuration of amplitude.

In the simulation environment, I sent a variety of stimulation configuration commands to the FPGA and observed the state of the output lines to the Stimulation Chip and Cross-Point Switch. The bit streams sent to the Stim Chip and CPS appeared to match the format required by each chip, so I proceeded to program the actual FPGA on the implant. In order to send commands to the FPGA, I first had to program the MCU.

4.1.2 Configuring the Stimulation Chip

Previous contributors to the project developed firmware for the MCU to send SPI commands to both FPGAs in the format specified in the previous section. I uploaded this firmware to the MCU and monitored the output of the Stim Chip by measuring the voltage across a resistor with an oscilloscope. I observed a stimulation waveform consistent with the stimulation parameters specified by the MCU. However, changing the stimulation parameters did not change the output from the Stim Chip. To debug, I monitored the SPI connection between the MCU and FPGA with a logic analyzer and found that the Master Out Slave In and the Master In Slave Out data lines were switched. I fixed this error in the pin configuration file for the FPGA and confirmed the change with the logic analyzer.

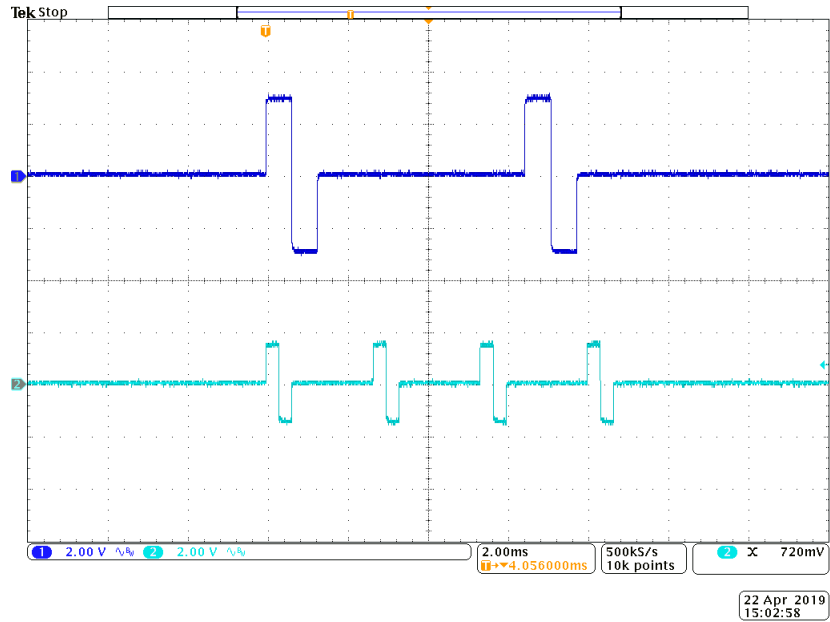


Figure 4-1: Oscilloscope shot of a typical stimulation with two active channels.

However, after attempting to initiate stimulation from the MCU once again, the stimulation output remained unchanged. Next, I monitored the SPI connection between the FPGA and the Stim Chip. After careful examination of the bit stream sent by the FPGA, I found fewer than the required number of bits to successfully program the Stim Chip. In the VHDL for the Stim Chip Engine on the FPGA, a counter limits the amount of data sent. After fixing this counter to send the correct number of bits, the Stimulation FPGA successfully programmed the Stim Chip to initiate stimulation. Figure 4-1 shows an example of two channels stimulating with different parameters.

4.1.3 Configuring the Stimulation Cross-Point Switch

After successfully configuring stimulation, I worked on configuring the Stimulation Cross-Point Switch (Stim CPS). The Stim CPS consists of 2 2x32 CPS but acts as one 4x32 CPS. Each CPS contains two registers. The first register controls the connection of 2 analog inputs to each of the 32 electrode pins. The second register controls the connections between the 32 electrodes and their corresponding recording connections. Both registers must be programmed to correctly configure the CPS.

I sent SPI commands from the MCU to the Stim FPGA to configure the Stim CPS and used an ohmmeter to test connections. The CPS did not change configuration. After monitoring the SPI connection, I determined that the data lines were switched, as they were with the Stim Chip. After modifying the FPGA pin configuration file and sending the full CPS configuration message, the connections behaved as expected.

4.2 Wireless Stimulation

After successfully implementing stimulation from the MCU, the major goal of the project was to initiate stimulation wirelessly. Both the MCU and BLE Chip serve as SPI masters to the Stimulation FPGA, so both chips can (potentially) send commands to initiate stimulation. To complete this phase in the simplest way, the BLE Chip must receive a command from the external transceiver BLE Chip and forward the command to the Stimulation FPGA. In this case, the MCU no longer sends commands to the FPGA and serves only to drive a clock used by the BLE Chip.

4.2.1 BLE Connection on Development Boards

The first step of this phase was to learn how to program two devices to initiate and sustain a BLE connection. To simplify development, I first experimented with two BLE development boards using the same chip as the implant.

Every BLE devices acts in one of four specific roles: broadcaster, observer, peripheral, or central. A broadcaster sends advertisements but is unable to connect, and an observer receives advertisements and is also unable to connect. A peripheral sends advertisements and is able to accept a connection, and a central receives advertisements and is able to initiate a connection. Each of these roles is defined in a particular layer of the BLE stack called the Generic Access Profile (GAP) layer. In the case of the neuromodulation system, the implants act as peripherals and the external transceiver acts as a central.

To establish a connection between a central and a peripheral, the peripheral first sends out advertisements that are configured to be "connectable." Meanwhile, the

central scans for advertisements. Once the central detects an advertisement from the peripheral, the central can send a request to connect to the peripheral. Depending on its configuration, the peripheral accepts the connection request. Next, the central initiates the first connection event. Connection events occur at a specified interval (the connection interval), and BLE devices only exchange information at connection events. The connection interval must be set between 7.5 ms and 4 s. The connection interval is one of the primary ways that BLE reduces power consumption compared to a protocol where data streams continuously. BLE devices send data relatively infrequently, so the BLE stack turns the radio off between connection events to save power. Consequently, longer connection intervals reduce power consumption, although this is at the expense of throughput.

At each connection interval, the master device (central) transmits data to the slave device (peripheral), and the slave transmits data back to the master. This exchange is necessary in order to keep the BLE connection active. If the slave has no data to send back to the master, it must still transmit an empty packet. Otherwise, the connection may time out.

To establish a BLE connection between the two BLE development boards, I used two example projects for the BLE peripheral and BLE central provided by the manufacturer.

4.2.2 BLE Connection with the Implant

After establishing a connection between two development boards, I worked to establish a connection between a development board and the implant. While the implant and development boards use the same chip, the implant uses a version of the chip that is housed in a different package, so it required a unique configuration of the code.

I first modified the board files in the BLE peripheral example project to work with the chip package used on the implant. This required removing several non-existent pins, modifying SPI connections to match the implant schematic, and disabling features supported by the development board but not by the implant. Additionally, I modified the peripheral project to allow the implant BLE Chip to operate using

the internal 32 kHz oscillator rather than an external oscillator. This required a few modifications to the example project to enable calibration of the internal oscillator which is less precise than an external oscillator. After making these modifications, I tested the project once again on the development board. These modifications did not make the project incompatible with the development board, and the board successfully established a connection with the BLE central. Next, I uploaded the BLE peripheral firmware to the implant and established a connection with the central BLE development board.

4.2.3 SPI Connection with BLE

Establishing a BLE connection with the implant verified that the BLE Chip on the implant was fully functional. Next, I worked to send data through the BLE connection to configure stimulation. Previous contributors to the neuromodulation project developed two BLE projects to test the throughput of BLE connections between one central device and four peripheral devices. The projects sent SPI data from the central to each of four peripherals in sequence. I modified the peripheral project to work with the actual implant and managed to send data through the BLE connection from the central to the peripheral. I fed SPI data into the BLE central (with an Arduino) but received incorrect data on the SPI output of the implant. After modifying the BLE transmission unit size, changing SPI parameters to interface correctly with the Stimulation FPGA (correct message length and baud rate) and changing the way the program packaged BLE data for SPI transmission, I successfully configured the Stim Chip through BLE.

Unfortunately, the BLE connection between the BLE central and the implant only persisted long enough to send one stimulation command. I found that a certain SPI function in the BLE peripheral code took too long to execute, causing the BLE connection to time out. I modified the timeout interval of the BLE connection and eliminated the bottleneck in the SPI function, and the BLE connection no longer dropped. Lastly, I iterated through a wide variety of Stim Chip commands and CPS commands to confirm the full functionality of the BLE connection.

Chapter 5

Measurements

5.1 Stimulation Latency

For certain applications of the implant, it is critical to minimize latency. For example, if the implant is configured to deliver a certain stimulation in response to a given recorded waveform, the latency from the initial recording to the delivery of stimulation must be as small as possible. However, latency with BLE is inherently non-deterministic. The peripheral and slave devices connect at a pre-determined interval known as the "connection interval." Once the devices are connected and this interval is established, the two devices exchange communications once every interval period. The allowable range of the connection interval is 7.5ms to 4s. Setting a shorter connection interval allows for lower latency, but the devices will consume more power. Setting a longer interval reduces power consumption at the expense of latency. The relationship between power consumption and latency is explored further in 5.2.3. The connection events are handled by a low-level layer in the BLE stack, so latency varies with each transmitted packet. The time it takes for a packet to transfer between two BLE devices depends on where the devices are in their connection interval when the packet attempts to send.

In order to characterize the latency of stimulation delivery, I measured the interval between a command originating from the external transceiver and the resulting stimulation on the implant. I monitored these two signals on an oscilloscope, and

Table 5.1: Latency with Varying Connection Intervals

| Connection Interval (ms) | Mean Latency (ms) (n=100) | Std Dev |
|--------------------------|---------------------------|---------|
| 10 | 21.2 | 6.9 |
| 50 | 42.9 | 16.9 |
| 100 | 66.9 | 30.3 |

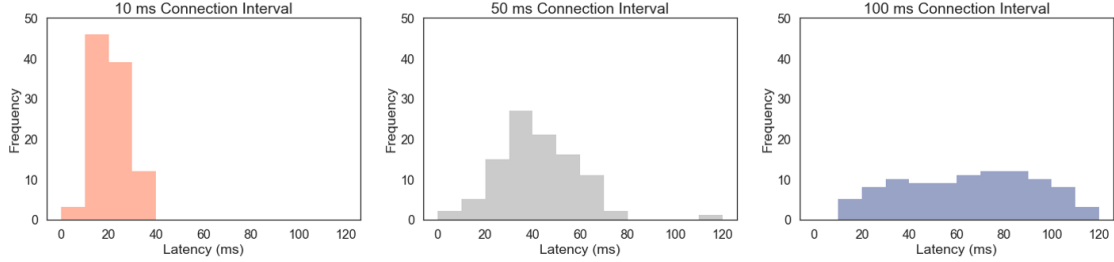


Figure 5-1: Latency Distributions for Various Connection Intervals

added an automated measurement of the delay between the first rising edge of the external transceiver signal and the first rising edge of the resulting stimulation. The external transceiver signal is a 20-byte SPI message sent with a baud rate of 1 Mbps, so message takes only 0.16 ms to transmit. The duration of this message is significantly shorter than the shortest possible latency (7.5 ms), so the delay between the start and end of the SPI message can be neglected.

The latency varies with each packet sent, so I collected 100 measurements to create a latency distribution. I repeated this experiment with 3 different connection intervals: 10 ms, 50 ms, and 100 ms. A summary of the measurements is provided in Table 5.1, and the distributions of each experiment are provided in Figure 5-1.

5.2 Power Consumption

Power management is critical in implanted medical devices in order to avoid overheating and, in some cases, to optimize battery life. While the implant does not have any form of energy storage, the device can only dissipate a certain amount of heat before causing damage to the patient. In an effort to characterize the power consumption of the implant at this stage, I measured the power consumed by the neuromodulation

system in a variety of configurations.

5.2.1 Power Consumption by Component

The implant development board incorporates removable jumpers to enable or disable power to every major component, including voltage regulators. The power delivery system for the implant is somewhat complicated, and there are many dependencies between components. For example, the BLE chip requires the MCU to provide a clock signal, so the power consumption of the BLE chip cannot be measured accurately if the MCU is disabled. Further, the development board takes a 5V input and converts it to +9V, -9V, 3.3V, 2.5V, 1.8V, and 1.2V to supply all of the components on board with power and reference voltages. Four linear regulators provide the voltages below 5V, and they are less efficient at lower loads. If we disable components and reduce the load on any given regulator, the regulator consumes more power. Further, disabling a component does not necessarily mean the component consumes zero power. Certain components, like the Amplifier and ADC Chip, have pull-up resistors permanently tied to voltage supplies. Even when the input voltage to the Amp/ADC is zero, the resistors consume several mW. Consequently, the difference in total power when disabling a component on the board cannot be attributed entirely to the component itself. For these reasons, we cannot simply measure power consumption by selectively enabling and disabling components.

In order to measure the power of each component, I measured the voltage and current into each component individually using a voltmeter and ammeter, respectively. For components that do not supply power to any other part of the board (i.e. all components that are not voltage regulators), I considered all of the power into a component as power consumed by that component. For the voltage regulators, I measured the voltage and current into the regulator and the voltage and current out of the regulator. To calculate power dissipated by the regulators, I took the difference between the power in and the power out. I configured the board specifically for stimulation, so components involved in recording were disabled and are not reported. The results of these measurements are provided in Table 5.2.

Table 5.2: Power Consumption by Component (Idle State)

| Component | Power Consumed (mW) | Voltage In (V) | Current In (mA) | Power In (mW) | Voltage Out (V) | Current Out (mA) | Power Out (mW) |
|------------------|---------------------|----------------|-----------------|---------------|-----------------|------------------|----------------|
| Stimulation FPGA | 3.56 | 1.2 and 1.8 | 2.92 | 3.56 | 0 | 0 | 0 |
| BLE Chip | 0.66 | 1.8 | 0.37 | 0.66 | 0 | 0 | 0 |
| Microcontroller | 3.15 | 1.8 | 1.75 | 3.15 | 0 | 0 | 0 |
| Stim Chip | 0.05 | 1.8 | 0.03 | 0.5 | 0 | 0 | 0 |
| 1.8V LDO | 7.28 | 4.72 | 2.43 | 11.47 | 1.8 | 2.33 | 4.19 |
| 1.2V LDO | 13.67 | 4.72 | 3.68 | 17.38 | 1.2 | 3.09 | 3.71 |

These measurements show the power consumed by each component in an idle state. In other words, the neuromodulation system is neither recording nor stimulating. Further, none of the components have been optimized to minimize power consumption. Recommendations for reducing power consumed by the MCU are provided in 6.3.

5.2.2 Power Consumption with Varying Stimulation Parameters

After optimizing each component to reduce power consumption, we expect the Stimulation Chip to consume the most power. In order to characterize the power consumption of this component, I measured the current drawn by the implant in a variety of stimulation configurations. The implant is not yet optimized to reduce power consumption, so the total power consumed in each stimulation state is not particularly informative. To account for this, I compared each stimulation configuration to a baseline power consumption. I alternately sent continuous stimulation commands and halting commands in 10 second intervals and monitored the current drawn on a real-time plot. Each stimulation command configured the Stim Chip to deliver a continuous train of 200 μs wide pulses at a specific frequency and amplitude. A pulse width of 200 μs is fairly standard for nerve stimulation. Frequencies ranged from 25 to 100 Hz, and stimulation current amplitudes ranged from 1 mA to 10 mA. Measurements were repeated with 1 channel stimulating and 2 channels stimulating. These measurements are reported in Table 5.3 and plotted in Figure 5-2.

As expected, stimulations with higher amplitudes and higher frequencies consumed more power. Further, 2 channel stimulation consumed twice as much power as

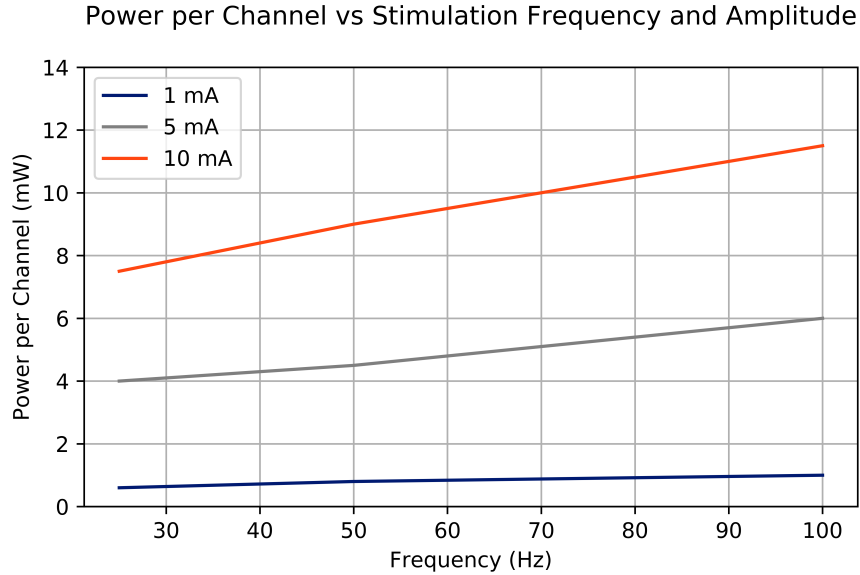


Figure 5-2: Power consumption per channel at various stimulation frequencies and amplitudes

1 channel stimulation in every configuration, as expected. The maximum power from 1 channel stimulation was 11.5 mW. Stimulation amplitudes below 1 mA yielded imperceptible differences in power consumption given the precision of the source meter used to gather these measurements.

5.2.3 Power Consumption with Varying BLE Connection Intervals

In addition to varying stimulation parameters, I monitored power consumption for different BLE connection intervals. As a baseline, I measured power consumption with the BLE chip disabled. With BLE enabled, I gathered measurements with connection intervals of 10 ms, 50 ms, and 100 ms. These measurements are reported in Table 5.4. As expected, shorter connection intervals increase power consumption. Lastly, I measured power consumption of only the BLE Chip when connected versus power consumption while disconnected. The BLE Chip consumed up to 0.66 mW while disconnected and up to 3.5 mW while connected with a connection interval of 10 ms.

Table 5.3: Power Consumption with Varying Stimulation Parameters

| No. Channels | Amp (mA) | Freq. (Hz) | Idle Current (mA) | Stim Current (mA) | Current Diff (mA) | Power (mW) |
|--------------|----------|------------|-------------------|-------------------|-------------------|------------|
| 1 | 1 | 25 | 45.5 | 45.62 | 0.12 | 0.60 |
| 1 | 1 | 50 | 45.5 | 45.66 | 0.16 | 0.80 |
| 1 | 1 | 100 | 45.5 | 45.7 | 0.20 | 1.0 |
| 1 | 5 | 25 | 45.5 | 46.3 | 0.8 | 4.0 |
| 1 | 5 | 50 | 45.5 | 46.4 | 0.9 | 4.5 |
| 1 | 5 | 100 | 45.5 | 46.7 | 1.2 | 6.0 |
| 1 | 10 | 25 | 45.5 | 47 | 1.5 | 7.5 |
| 1 | 10 | 50 | 45.5 | 47.3 | 1.8 | 9.0 |
| 1 | 10 | 100 | 45.5 | 47.8 | 2.3 | 11.5 |
| 2 | 1 | 25 | 45.5 | 45.78 | 0.28 | 1.4 |
| 2 | 1 | 50 | 45.5 | 45.84 | 0.34 | 1.7 |
| 2 | 1 | 100 | 45.5 | 46 | 0.5 | 2.5 |
| 2 | 5 | 25 | 45.5 | 47.1 | 1.6 | 8.0 |
| 2 | 5 | 50 | 45.5 | 47.3 | 1.8 | 9.0 |
| 2 | 5 | 100 | 45.5 | 47.85 | 2.35 | 11.75 |
| 2 | 10 | 25 | 45.5 | 48.6 | 3.1 | 15.5 |
| 2 | 10 | 50 | 45.5 | 49.1 | 3.6 | 18.0 |
| 2 | 10 | 100 | 45.5 | 50.15 | 4.65 | 23.3 |

Table 5.4: Power Consumption with Varying BLE Connection Intervals

| Conn. Interval (ms) | No. Channels | Amp (mA) | Freq. (Hz) | Idle Current (mA) | ΔI from Non-BLE (mA) | Power (mW) |
|---------------------|--------------|----------|------------|-------------------|------------------------------|------------|
| 10 | 1 | 10 | 100 | 38.55 | 0 | 0 |
| 50 | 1 | 10 | 100 | 36.84 | 0 | 0 |
| 100 | 1 | 10 | 100 | 38.55 | 0 | 0 |

Chapter 6

Future Work

6.1 Security

With the growth of the "Internet of Things," security is a looming concern. While the implant has no direct connection to the internet, the presence of a BLE connection poses security concerns because many modern devices can form BLE connections. As an initial precaution, both the implant and the external transceiver contain "whitelists" on their BLE Chips that restrict their connectivity to other devices. As configured, the implant and external transceiver can only connect to each other. Further work should also consider implementing encrypted BLE communication, although this will affect the speed of communication.

In guarding against potential threats to security, we must consider the consequences of a breach occurring. Assuming the implant is placed properly in a patient, can it be configured in such a way to harm the patient? Further work might introduce safeguards to authenticate any attempt to reprogram the implant and incorporate hard limits on the range of stimulation depending on use case. For example, in a use case that never requires more than 1 mA stimulation, the implant should limit stimulation output to 1 mA regardless of programming. We cannot necessarily anticipate every possible security threat, so it is best to incorporate security features preemptively.

6.2 Alternatives to BLE

While the neuromodulation system currently uses BLE for communication from the external transceiver to the implant, BLE is not necessarily the best option. BLE offers low power consumption at the expense of low throughput and long (and uncertain) latency. Other wireless technologies may prove better suited to the neuromodulation system depending on the application. A faster technology might be able to replace both the Draper Radio and the BLE Chip, reducing the complexity of the system and potentially reducing the size. Communication between the implant and the external transceiver is across a very small distance (through the skin), so forms of inductive data transfer might also prove useful. Figure 6-1 compares a variety of wireless communication protocols based on data rate and transmitting power consumption [17, 18, 19, 20, 21, 22, 23, 24, 25, 26, 27, 28, 29, 30, 31, 32, 33].

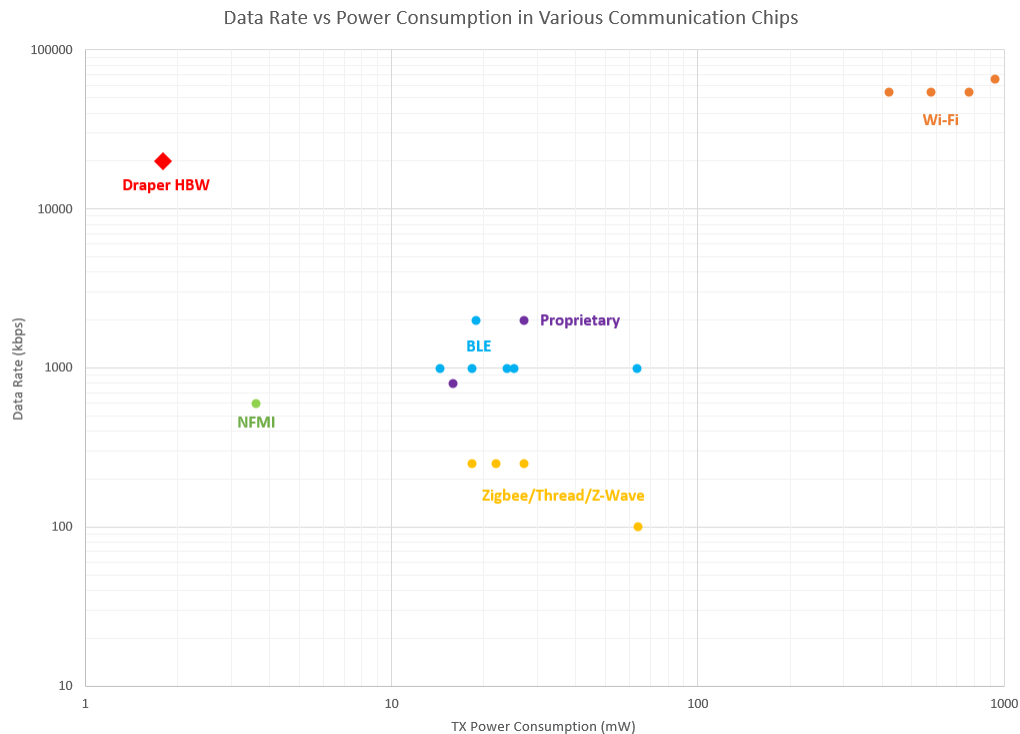


Figure 6-1: Comparison of power consumption and data rate of various wireless protocols

6.3 Reducing Power Consumption

In order to reduce the power consumption of the implant, we must optimize each component individually. Of the major components in the implant, we have the most control over the MCU, BLE Chip, and FPGAs. The MCU in the implant offers a number of low power states. Further work should configure the MCU to enter a low power state or standby state during periods of inactivity and disable all non-essential input and output pins. For example, the MCU might be configured to wake on an interrupt from the BLE Chip and otherwise remain in a sleep mode. To reduce power consumed by BLE communication, the BLE Chip should remain disconnected from the external transceiver whenever possible. The BLE Chip can be configured to wake periodically to advertise for a connection. Lastly, the FPGAs can be configured to operate at lower frequencies and to enter low power states when inactive.

Bibliography

- [1] NeuroPace Inc. The RNS System. Website.
https://www.neuropace.com/the-rns-system/?gclid=EAIaIQobChMIgd25-0bd3QIVwp6zCh0kkgLLEAAYASAAEgLfavD_BwE.
- [2] Nevro Corp. Why hf10 overview. <https://www.hf10.com/why-hf10/overview/>.
- [3] Draper. A tiny neural implant even your brain can love. Website, 2018.
<https://www.draper.com/news-releases/tiny-neural-implant-even-your-brain-can-love>.
- [4] Philip L. Gildenberg. Neuromodulation: A historical perspective. In P.H. Peckham E.S. Krames and A.R. Rezai, editors, *Neuromodulation*, chapter 2. Elsevier Ltd., 2009.
- [5] S. Thomson. History of neuromodulation. Website, 2010.
<https://www.neuromodulation.com/history-of-neuromodulation>.
- [6] L. McLellan J. Brice. Suppression of intention tremor by contingent deep-brain stimulation. *Lancet*, 1980.
- [7] International Neuromodulation Society. Neuromodulation therapies. Website, 2018. <https://www.neuromodulation.com/for-medical-providers>.
- [8] LivaNova Inc. Vns therapy. Website, 2018.
<https://us.livanova.cyberonics.com/home>.
- [9] Abbott. St. jude medical infinity dbs ipg. Website, 2016.
<https://www.neuromodulation.abbott/us/en/hcp/products/dbs-movement-disorders/st-jude-medical-infinity-dbs-system.html>.
- [10] Medtronic. Deep brain stimulation systems. Website, 2018.
<https://www.medtronic.com/us-en/healthcare-professionals/products/neurological/deep-brain-stimulation-systems.html>.
- [11] Boston Scientific Corp. Spinal cord stimulator systems. Website, 2016.
<https://www.bostonscientific.com/en-US/products/spinal-cord-stimulator-systems.html>.

- [12] Medtronic. Spinal cord stimulation systems. Website, 2018. <https://www.medtronic.com/us-en/healthcare-professionals/products/neurological/spinal-cord-stimulation-systems.html>.
- [13] Abbott. Spinal cord stimulation. Website, 2016. <https://www.neuromodulation.abbott/us/en/hcp/products.html>.
- [14] J. Sanchez. Systems-based neurotechnology for emerging therapies (subnets). Website, 2018. <https://www.darpa.mil/program/systems-based-neurotechnology-for-emerging-therapies>.
- [15] National Institutes of Health. Stimulating peripheral activity to relieve conditions. Website, 2018. <https://commonfund.nih.gov/sparc>.
- [16] Blackrock Microsystems. Utah array. Website, 2018. <https://blackrockmicro.com/electrode-types/utah-array/>.
- [17] Texas Instruments. *TRF7970A*.
- [18] ST. *CR95HF*.
- [19] Nordic. *nRF8001*.
- [20] Dialog. *DA14580*.
- [21] Texas Instruments. *CC2640*.
- [22] Cypress. *PSoC 4100 BLE*.
- [23] Microsemi. *ZI70102*.
- [24] Silicon Labs. *EFR32FG1*.
- [25] Texas Instruments. *CC3220R*.
- [26] Espressif. *ESP8266*.
- [27] Cypress. *CYW43362*.
- [28] Qualcomm. *AR6004*.
- [29] Texas Instruments. *CC2630*.
- [30] NXP. *NXH2261UK*.
- [31] NXP. *MKW41Z*.
- [32] Silicon Labs. *MGM111*.
- [33] Silicon Labs. *ZM5101*.